JOURNAL OF TECHNIQUES

Journal homepage: http://journal.mtu.edu.iq

RESEARCH ARTICLE - ENGINEERING

Position - Velocity Control for Two PMDC Motors Connected by a Cross-Coupling Technique with Butterflies Optimization Algorithm

Kareem Ghazi Abdulhussein[1*], Naseer M. Yasin[1], Ihsan J. Hasan[1]

[1] Department of Electrical Power Engineering Techniques, Middle Technical University, Iraq.

* Corresponding author E-mail: engkarim1984@gmail.com

Article Info.

Article history:

Received
02 April 2021

Accepted
11 May 2021

Publishing
30 June 2021

Abstract

In this paper, two contributions are presented. the first is to design two cascade controllers to control the velocity and position for two Permanent Magnet DC motors (PMDC) working together at the same time for use in many applications such as CNC machines, robotics, and others. Furthermore, the cross-coupling technique is used to connect these motors and adjust the precise synchronization of their movement on the axes. The second contribution is the use of the butterfly's optimization algorithm (BOA) with the objective function Integral Time Absolute Error (ITAE) to extract the optimal parameter values for the two cascade controllers and the synchronization controller in order to obtain the best accurate results. The simulation results showed high accuracy to reach the desired position at a regular velocity of both the PMDC motors with accurate synchronization and tracking trajectory on the axes. In addition, a very small position deviation of 0.021 rad was observed, and the system returned to a steady-state after 2 seconds of applying the full load.

Keywords: PMDC Motor; cascade controller; BOA; cross-coupling technique; synchronization

1. Introduction

Recently, it has been noted that the interest of researchers, especially those working in the field of robotics, has increased in the subject of velocity control and the position of the permanent magnet DC motor due to its importance in many applications that require high accuracy with accurate tracking of the movement path to reach the specified position at a certain velocity[1].

The PMDC motor used in this paper is one of the special types of DC motors and it is similar in structure to the shunt-connected DC motor, but the difference between them is the use of permanent magnets to generate magnetic flux instead of generation by field windings[2,3].

This motor has many Applications such as using it with car front wipers and moving windows for cars and household appliances such as food mixers and others [4,5], in addition to the importance of using it in CNC machines, robotics, and electric vehicles[6,7].

Two cascade controllers have been used, one for each PMDC motor. This cascade controller consists of three controllers, the first for position control, the second for velocity control, and the third for current control where the current controller is designed as an inner loop, and both position and velocity are outer controllers [8] . P, PI, and PI controllers are used instead of a PID controller for the position, velocity, and current respectively [9] . The main reason for using the cascade controller is to reduce or reject disturbances to return the system to a steady-state [10 -12].

There are several techniques to synchronize the movement of PMDC motors on the axes and reduce the synchronization error between them, such as parallel, master-slave, Virtual line-shafting (VLS), biaxial controller, Cross-coupling controller (CCC), and deviation coupling controller[13 -17].

Nomenclature		**Symbols**	
PMDC	permanent magnet DC motor	E_a	electromotive force or back emf (v)
CNC	computer numerical control	K_t	torque constant (Nm / A)
PID	proportional–integral–derivative controller	K_v	back emf constant (v. sec / rad)
IATE	integral time absolute error	Va	nominal voltage (v)
PWM	pulse width modulation	TL	nominal load torque (Nm)
BOA	butterflies optimization algorithm	Vc	voltage control (v)
		L_a	armature inductance (H)
		R_a	armature resistance (Ω)

In this paper, a cross-coupling controller is used which consists of a controller type PD to adjust the synchronization of movement between the two PMDC motors.

To ensure the accuracy of the results, the butterfly optimization algorithm is used twice to extract the values of the P and PI parameters for the velocity, position, and current controls, and again to extract the values of the PD synchronization controller parameters. In both cases, the objective function (ITAE) is used to reduce the error ratio between input and output.

There are many previous researchers in the field of controlling the velocity and position of dual PMDC motors. For example, but not limited. In 2012 Vinayak Mhase, et al designed a system which consists of two controllers PD to control the speed, and PI controller to control the position of two DC on axes[18]. In 2013 Shih-Ming, et al Introduced a new master-slave method that is used to synchronizing the movement of two-drive systems and tested it on a gantry-type a two-axis platform[19]. Burak Sencer and Eiji Shamoto in 2014 Introduced a control system used to operate a gantry-type machine tool. It consists of two controllers for each PMDC motor, a PI controller for speed P controller for the position [17] . In 2017 Nishant Kumar and Tiwari presented a speed control system with a cross-coupling technique used to synchronizing movement for several DC motors. This controller consists of a non-linear PID controller[20] . Panlong Zhang and Zhongcheng Introduced 2019 a speed control system for a two-wheel independent DC motor for automatic guided vehicles and tested to move from one location to another [15]. In 2020 JongNam Bae et al presented a parallel position control system for dual DC motor with Hall sensor. The speed and position are estimated by using the back EMF compensator and the current model speed observer [6].

The main problem statement in this paper can be represented in two main problems, which are the design of a robust velocity-position control system for two PMDC motors working together and the other problem is the accurate synchronization of these motors' movement on the axes to reach the specified position.

To address these problems a cascade control system to control the velocity and position with BOA to extract the best values for the system (P,PI and PD) parameters and to solve the other problem which is the accurate synchronization, cross-coupling technique is used.

This paper is organized as follows: -

In the second section, the mathematical model of the PMDC motor and The general structure of the system with its simplification is explained, in the third section the cross-coupling technique is explained, in the fourth section the butterfly optimization algorithm and ITAE are explained, while the fifth section includes the results and discussion, and the last section includes the conclusion.

2. Mathematical Model

2.1. Mathematical Model of PMDC Motor

The equivalent circuit for a PMDC motor shown in Figure.1 consists of an armature circuit consisting of inductance (L_a) and resistance (R_a) connected on series. An electromotive force (E_a) is generated as a result of cutting the lines of flux generated by the permanent magnet, and it has a direction opposite to the direction of the source voltage. The mechanical part consists of moment inertia (J_m) and friction coefficient (B_m). The other parameters are torque constant (K_t) and back emf constant (K_v).

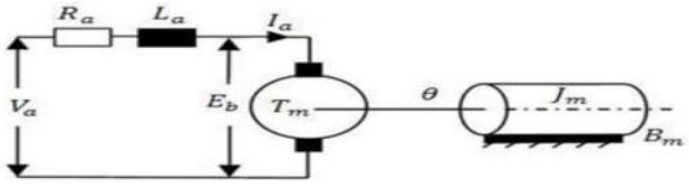

Fig. 1 Equivalent Circuit of Permanent-Magnet DC Motor [21]

The block diagram of the PMDC motor with the position output is shown in Figure 2.

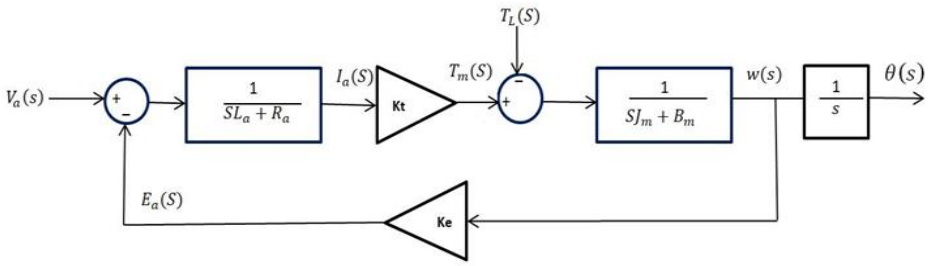

Fig. 2 Block diagram of Permanent-Magnet DC Motor [21,22]

From the block diagram above, The Mathematical Model of the PMDC motor with position output can be listed in the following equations [21,22].

$$\boldsymbol{v_a\,(t) = e_a\,(t) + R_a\,i_a\,(t) + L_a\,\frac{d}{dt}ia\,(t)} \quad (1)$$

$$\boldsymbol{e_a\,(t) = k_e\,\omega_m(t)} \quad (2)$$

$$\boldsymbol{T_m\,(t) - T_L\, = J_m\frac{d}{dt}\,\omega_m(t) + B_m\omega_m(t)} \quad (3)$$

$$\boldsymbol{T_m\,(t) = K_t i_a\,(t)} \quad (4)$$

By using Laplace transformation for the equations (1- 4) we obtain

$$\boldsymbol{V_a\,(s) = E_a(s) + R_a\,I_a(s) + SL_aI_a(s)} \quad (5)$$

$$\boldsymbol{E_a(s)\, = k_e\,\omega_m(s)} \quad (6)$$

$$\boldsymbol{T_m\,(s) - T_L\, = S\,J_m\omega_m(s) + B_m\omega_m(s)} \quad (7)$$

$$\boldsymbol{T_m\,(s) = K_t\,I_a(s)} \quad (8)$$

The overall transfer functions are defined for velocity and position control of the PMDC motor, respectively.

$$\frac{\boldsymbol{\omega_m(s)}}{\boldsymbol{V_a\,(s)}} = \frac{\boldsymbol{k_e}}{\boldsymbol{J\,L_aS^2 + (JR_a + BL_a)\,S + BR_a + k_e^{\,2}}} \quad (9)$$

$$\frac{\boldsymbol{\theta(s)}}{\boldsymbol{V_a\,(s)}} = \frac{\boldsymbol{k_e}}{\boldsymbol{J\,L_aS^3 + (JR_a + BL_a)\,S^2 + (BR_a + k_e^{\,2})S}} \quad (10)$$

Where k_e equal to K_t [23,24] and :

R_a = armature resistance (Ω)
Va = nominal voltage (v)
K_v = back emf constant (v. sec / rad)
L_a = armature inductance (H)
J_m = moment inertia (kg.m^2)
B_m = friction coefficient (Nm.s/rad)
E_a = electromotive force or back emf (v)
TL = nominal load torque (Nm)
ω_m = motor velocity (rad /sec)
θ(s) = Actual position (rad)
K_t = torque constant (Nm / A)

2.2. The General structure of the system

Figure 3 shows the general structure of the system, which consists of dual PMDC motors, and each motor has a cascade control with a reference signal in addition to an error synchronization controller connecting them together.

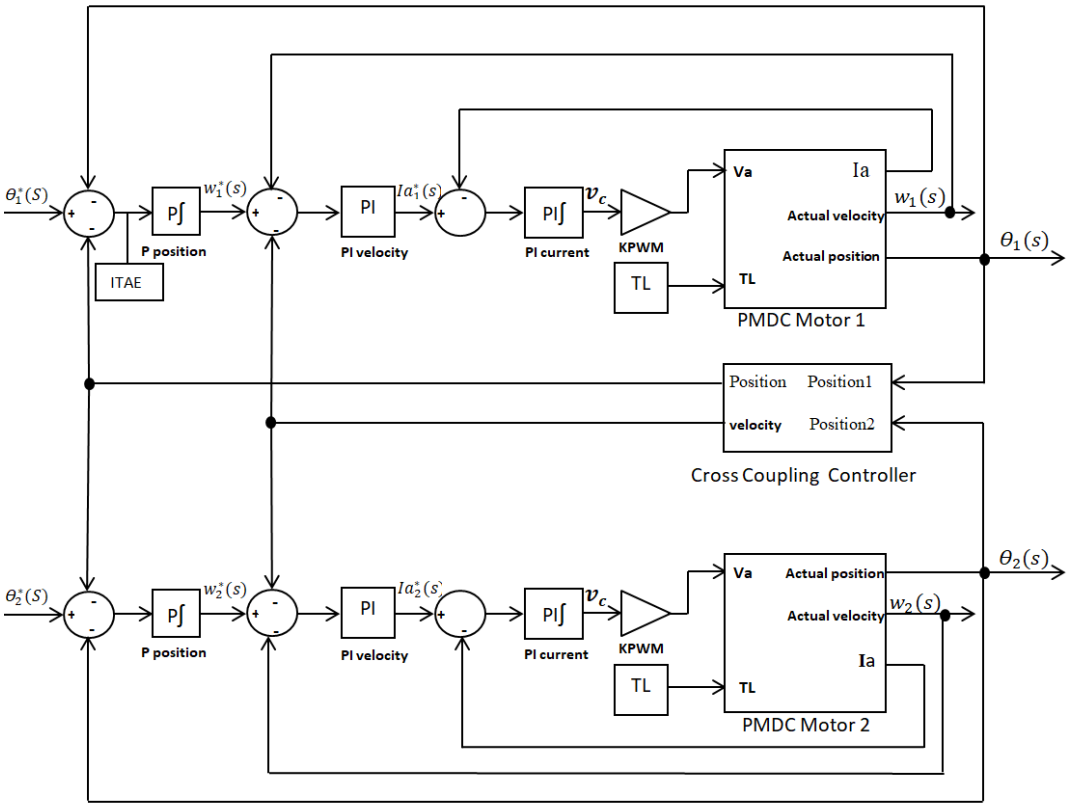

Fig. 3 General structure system

As shown in the figure above, the cascade control system consists of three controllers for current, velocity, and position. The reference signal enters the inner loop (i. e current loop) from the output of the velocity controller while the velocity reference signal enters from the output of the position controller so the input signal in the system is a position signal.
In this paper, the two PMDC motors have the same parameter values and Table 1 represents the values for these parameters.

Table 1 The PMDC Parameters [9]

Motor Parameters	value
Torque Constant	$K_t = 2.35 \quad Nm / A$
Armature Inductance	$La = 2.61 * 10^{-3}$ H
Armature Resistance	$Ra = 2.61\ \Omega$
Inertia of the Motor	$J_m = 0.068\ kg.m^2$
Friction Constant	$B_m = 0.008\ Nms/rad$
back emf constant	$K_v = 2.35 \quad Vs/rad$
Nominal Load	$T_l = 17.6$ Nm
Nominal Voltage	Va = 230 v

To simplify the system, it has been assumed that the input signal is the same for both motors, so the synchronization error becomes zero between them, and because the two motors have the same parameters, so the cascade control system can be simplified as follows: -

2.2.1. Simplify of Inner Loop

The inner loop as shown in Figure 4 consists of a PI controller where the reference current signal enters it from the output of the velocity controller.

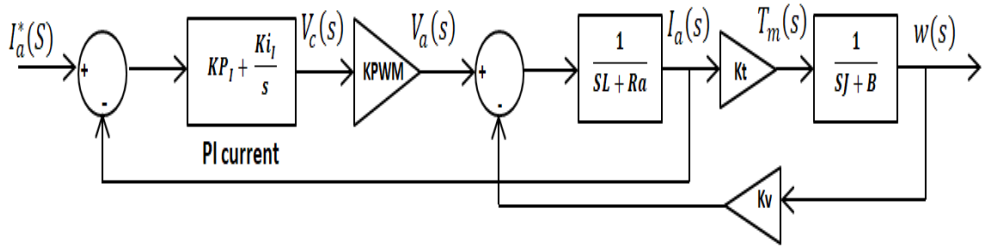

Fig. 4 Inner loop

A voltage control (vc) signal comes from the PI current controller and is compared with a triangular waveform signal. that is generated internally in the PWM circuit, producing a KPWM gain that simply represents the PWM controller and the dc-dc switching mode converter (i.e. H bridge) KPWM can be represented by the following equation in Laplace transform after making linearized of the dc-dc converter[24] .

$$V_a(s) = KPWM * V_c(s) \quad (11)$$

By neglecting the effect of the load torque, the inner loop can be simplified in Figure 5 (a) and (b)

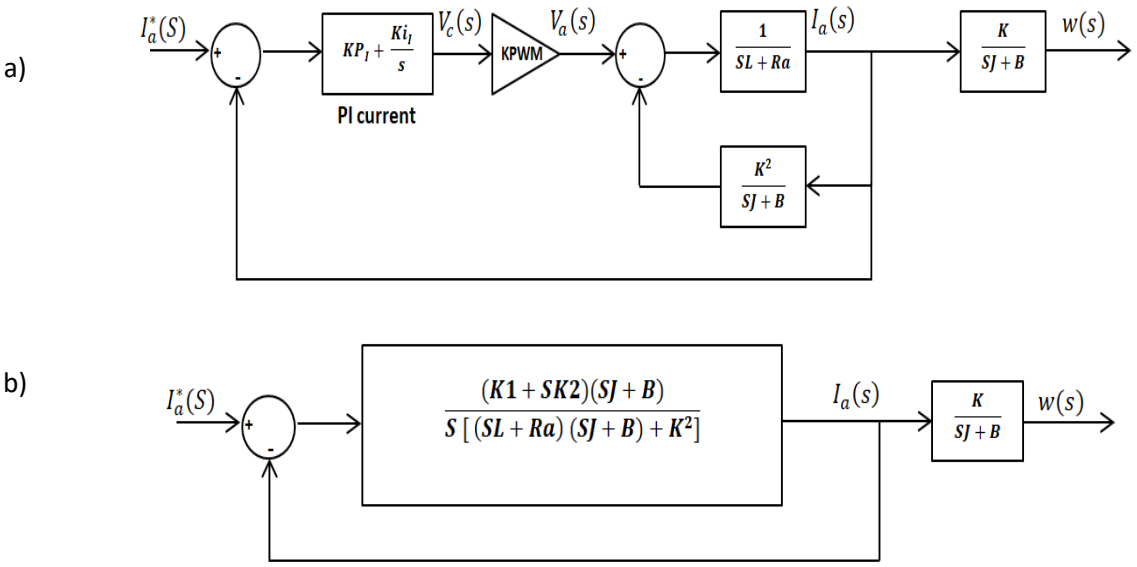

Fig. 5 (a) Simplification inner loop step one, (b) Simplification inner loop step two

Where

$$K = K_t = K_v \quad (12)$$

$$K1 = KPWM * Ki_I \quad (13)$$

$$K2 = KPWM * Kp_I \quad (14)$$

The inner loop transfer function can be represented by the following equation.

$$\frac{I_a(s)}{I_a^*(s)} = \frac{(K1+SK2)(SJ+B)}{S[(SL+Ra)(SJ+B)+K^2]+(K1+SK2)(SJ+B)} \quad (15)$$

2.2.2. Simplify of velocity loop

The velocity loop can be simplified in Figure 6 (a) and (b)

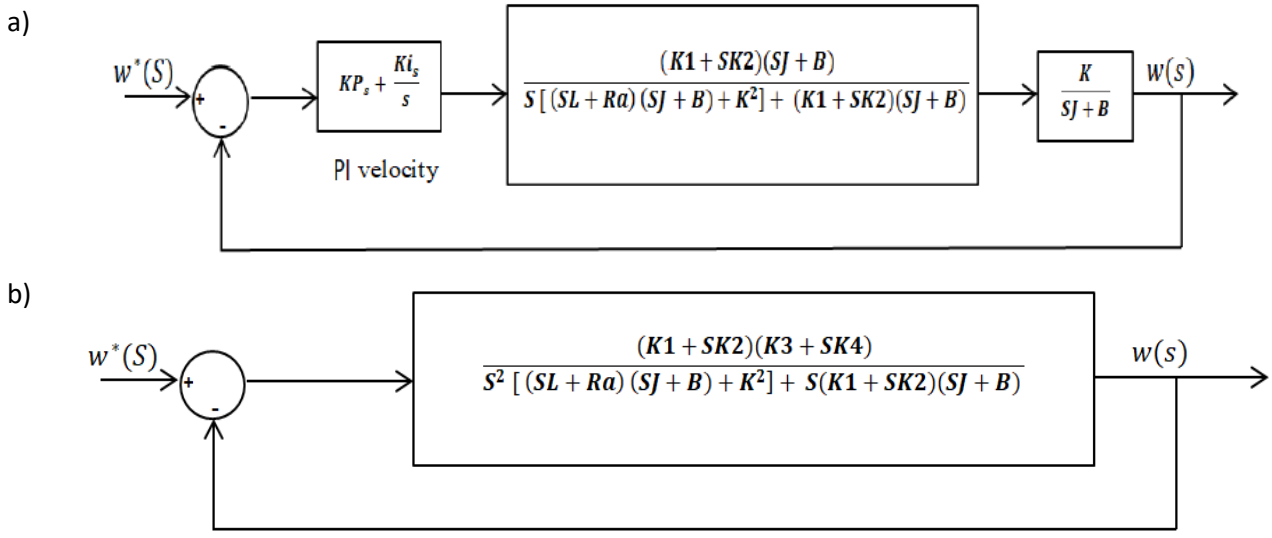

Fig. 6 (a) Simplification velocity loop step one, (b) Simplification velocity loop step two

Where

$$K3 = K * Ki_s \quad (16)$$

$$K4 = K * KP_s \quad (17)$$

The velocity loop transfer function can be represented by the following equation.

$$\frac{\boldsymbol{w_{(s)}}}{\boldsymbol{w^*_{(s)}}} = \frac{(\boldsymbol{K1+SK2})(\boldsymbol{K3+SK4})}{\boldsymbol{S^2\,[\,(SL+Ra)\,(SJ+B)+K^2]+\,S(K1+SK2)(SJ+B)+\,(K1+SK2)(K3+SK4)}} \quad (18)$$

2.2.3. Simplify of position loop

The position loop can be simplified in Figure 7 (a) and (b)

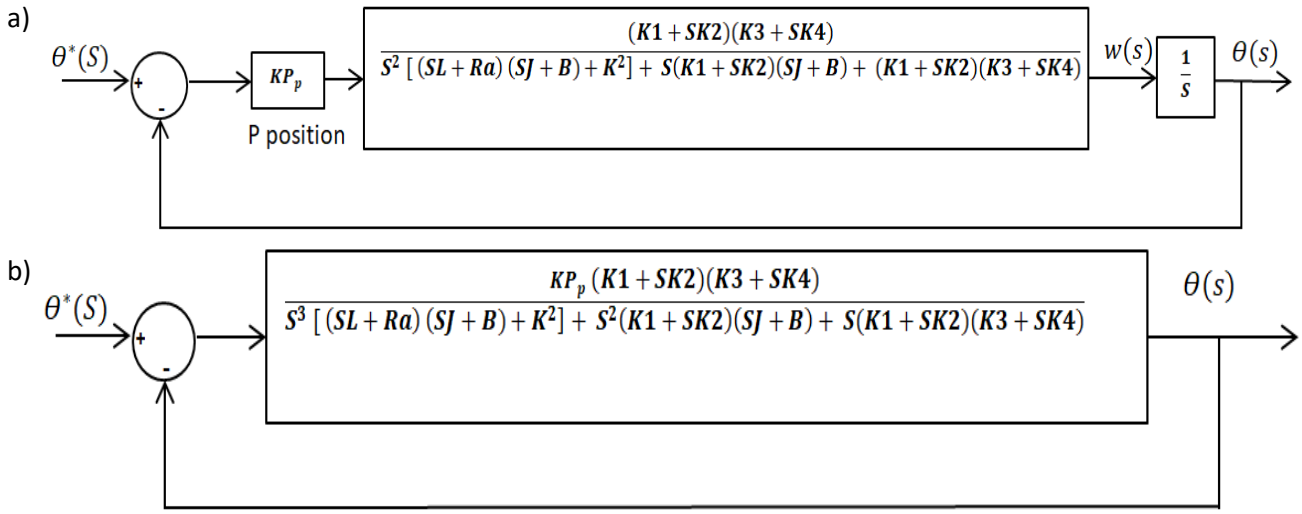

Fig. 7 (a) Simplification position loop step one, (b) Simplification position loop step two

The position loop transfer function can be represented by the following equation.

$$\frac{\boldsymbol{\theta_{(S)}}}{\boldsymbol{\theta^*_{(S)}}} = \frac{\boldsymbol{KP_p\,(K1+SK2)(K3+SK4)}}{\boldsymbol{S^3\,[\,(SL+Ra)\,(SJ+B)+K^2]+\,S^2(K1+SK2)(SJ+B)+\,S(K1+SK2)(K3+SK4)+KP_p(K1+SK2)(K3+SK4)}} \quad (19)$$

One of the benefits of the cascade control system, in addition to the benefits mentioned previously, is the ability to put limits on the reference signals for the system to protect the PMDC motor and the power electronic converter. In this paper, limits were placed on the velocity reference by an amount that does not exceed the rated motor velocity, which is 97.5 r.p.s, as well as limit, was placed on the reference voltage coming out of the PI current by 5v, which represents the control voltage (Vc) and is compared with a triangular voltage as explained above [24].

3. Cross-Coupling Technique

The cross-coupling technique, as introduced by Koren (1980) and Tomizuka et al. (1992), which is mainly used to solve the problem of non-synchronization of multi-motor caused by the influence of external factors and it provides advantages to improve synchronization performance for the movement along the axes [25] .
Several controllers have been used to create a synchronization controller relative to the input signal, whether velocity, position, or both. In this paper, a simple PD controller was used as shown in Figure (8).

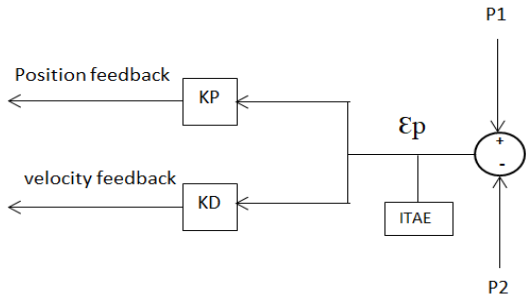

Fig. 8 PD synchronization control

The idea of this controller is to return an actual position from the first motor P1 and from the second motor P2 and then calculate the synchronization error from the following equation [25] .

$$\mathcal{E}p = c_1 e_1 - c_2 e_2 \quad (20)$$

Where

c_1, c_2 = cross-coupling parameters

e_1, e_2 = velocity errors for PMDC 1 and PMDC 2 Which can be represented by the following equation

$$e = w_r - w_a$$

Where

w_r = Reference velocity

w_a = Actual velocity

If the synchronization error $\mathcal{E}p = 0$ the synchronization goal is achieved and this was observed in the results seen Figure 15.
The reason for choosing a PD controller is that it contains the derivative which gives velocity after multiplying it by the position resulting from the synchronization error.

4. Butterflies Optimization Algorithm and ITAE

In this paper, a new metaheuristic algorithm taken from nature called the Butterflies Optimization Algorithm (BOA) is used. This algorithm is based on the principle of searching for food and mating between butterflies, as it uses chemical sensors (i.e. sensory receptors) to find food by smelling the nectar [27,28]. When the butterfly moves from one region to another, it generates a fragrance of different intensity according to the situation and spreads across this region. After spreading the fragrance, other butterflies can sense it and follow it, and in this way, the butterflies communicate with each other [27,28].

The entire concept of feeling and dealing with smell in butterflies is based on three main terms:

1- The sensory modality, denoted by the symbol c, and its value between [0-1].

2- Stimulus intensity, denoted by the symbol I.

3- The size of the stimulus or force on which the butterfly depends. It is known as power exponent and It is denoted by the symbol a and its value is between [0-1].

Two important issues on which the natural phenomenon of butterflies depends, namely the difference in the intensity of the fragrance and the formulation of the fragrance's function. The function of the fragrance can be represented according to the following equation

$$f = cI^a \quad (21)$$

When the butterfly smells the scent from another butterfly, it will move towards it. This stage is known as the global search and can be represented by equation (22) .

When the butterfly is not able to sense any smell coming from other butterflies, it will move randomly, and this movement is called local search and can be represented by equation (23).

$$X_i^{t+1} = X_i^t + \left(r^2 * g^* - X_i^t \right) * f_i \quad (22)$$

$$X_i^{t+1} = X_i^t + \left(r^2 * X_j^t - X_k^t \right) * f_i \quad (23)$$

Where

X_i^{t+1} = new solution vector ; X_i^t = solution vector

r = rondom number(n)between [0 , 1] ; g = current best solution

t = iteration number ; i = butterfly

X_j^t & X_k^t are jth and kth butterflies from the solution space

f_i = the perceived magnitude of the fragrance

Butterflies can change their movement randomly or move towards the best other butterfly, meaning that they have a decision to switch from local to global search, or vice versa. This transformation is called the probability switch and is denoted by the symbol ρ.

Figure 9 represents the approximate flowchart for BOA.

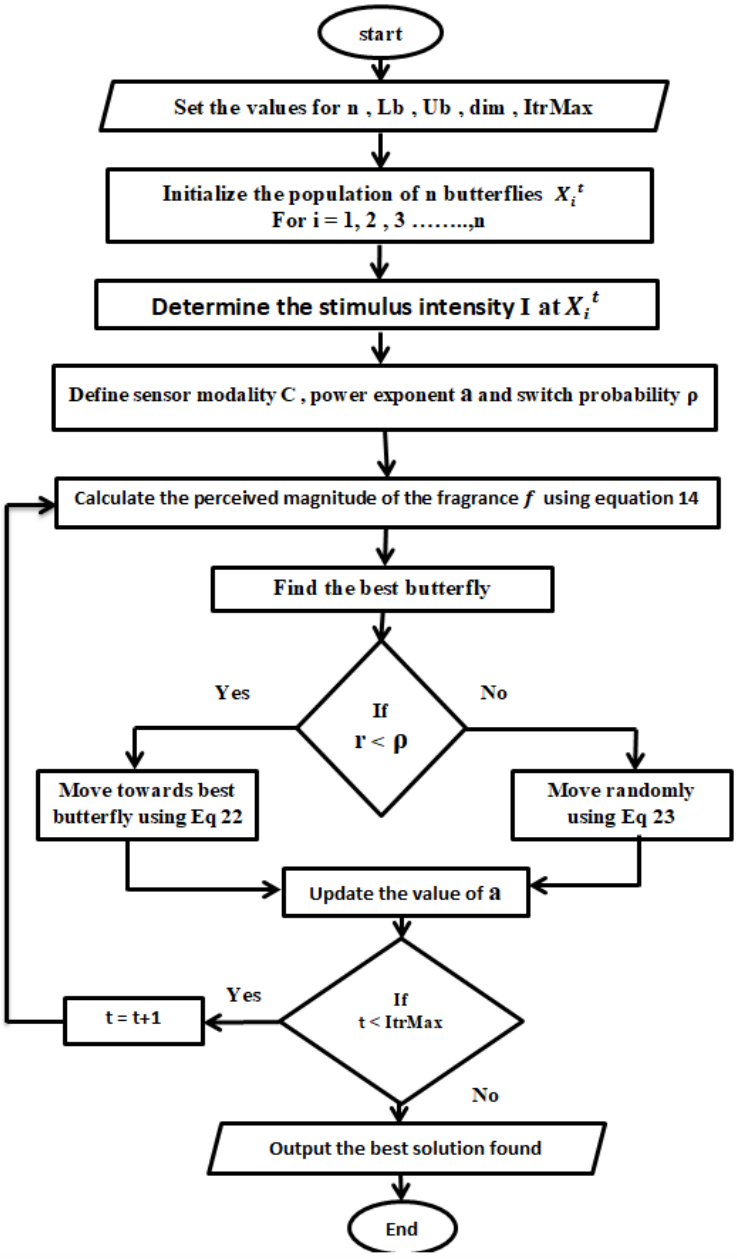

Fig. 9 BOA flowchart

In this paper, BOA is used in two cases:

Case 1: The BOA is used to extract the cascade P and PI parameters for One PMDC without connecting the synchronization error controller. Since the parameters of the two PMDC motors are the same so the same optimal parameters extracted can be used for both. These parameters gave satisfactory results for controlling the velocity and position of the PMDC motor (see Fig 3 location of ITAE).

Case 2: The BOA is used to extract the parameters of the PD synchronization error controller, as well as these parameters, gave satisfactory results after several attempts (see Fig 8 location of ITAE).

Tables 2 and 3 show the BOA parameters for both cases.

Table 2 BOA parameters for case 1

Parameters	values
Max iteration	5
No. search agents	20
No. dimension	5
probability switch ρ	0.8
sensory modality c	0.01
power exponent a	0.1
LB , UB	0 , 400

Table 3 BOA parameters for case 2

Parameters	values
Max iteration	5
No. search agents	20
No. dimension	2
probability switch ρ	0.8
sensory modality c	0.01
power exponent a	0.1
LB , UB	0 , 1

When designing any complex system, certain criteria must be chosen to give the best performance. These criteria are known as performance indices and there are many types of them. The function used in this paper is IATE, and it is represented by the following equation.

$$\text{ITAE} = \int_0^\infty t|e(t)|dt \quad (24)$$

5. Results and Discussion

The system is tested using the MATLAB environment, in both load and no-load cases. According to the general structure of the system shown in Fig. 3, PMDC 1 moves along the X-axis while PMDC 2 moves along the Y-axis. In addition, the system is tested when the reference position is single or multiple signals.

Table 4 represents the parameter values extracted using the BOA algorithm for both the PID cascade controller and the PD synchronization error controller.

Table 4 Parameters values

Cascade P and PI parameters	Value	Synchronization parameters	Value
KP position	0.899	KP position feedback	0.000001
KP velocity	315.5583	KD velocity feedback	0.01548
KI velocity	141.918		
KP current	273.3044		
KI current	0.0236		

The following figures show a description of all the above-mentioned cases as follows: -

1- Single input position reference at no-load case

Figure 10(a) shows the actual position in the case of no-load and single-input where the PMDC 1 moves by 8 rad on the x-axis while the PMDC 2 moves by 5 rad on the y-axis to reach the specified position (8,5) at the same time on the X-Y graph as shown in the figure 10(b). This is an indication of the robustness of the cascade controller and the synchronization error controller.

On the other hand, Figure 10(c) shows the velocity of the PMDC motors at no-load as the PMDC 1 motor is moving at 7.48 rad/sec, the PMDC 2 motor is moving at 4.8 rad/sec.

Both motors stop running at the same time when they reach the specified position. This is also an indication of the precise synchronization of the movement on the axes. The lower velocity values are due to the low reference position value.

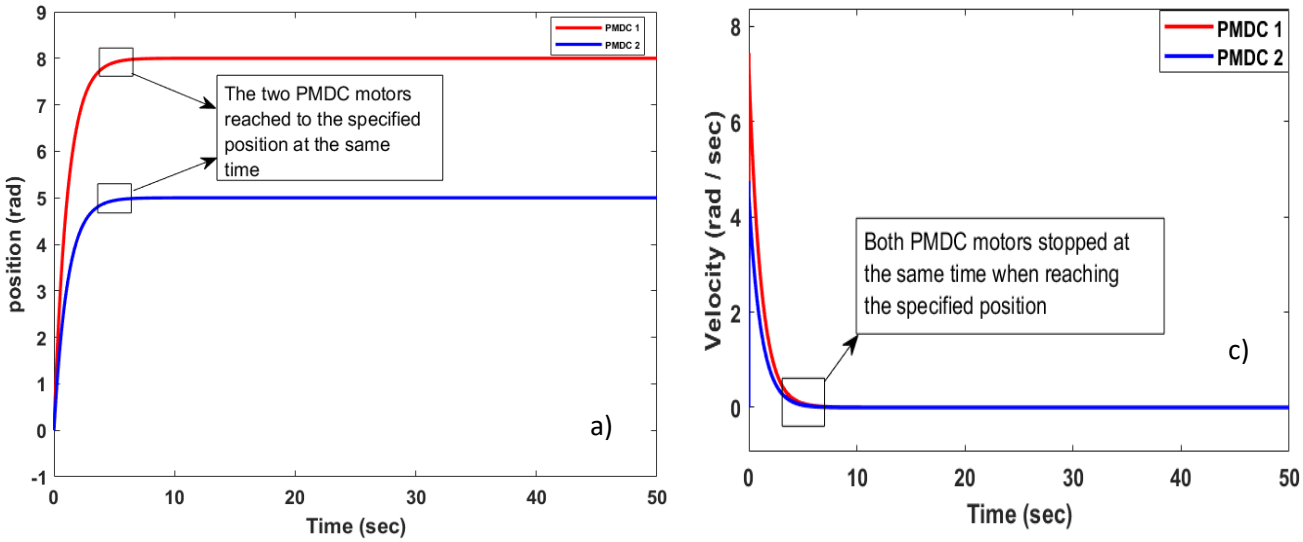

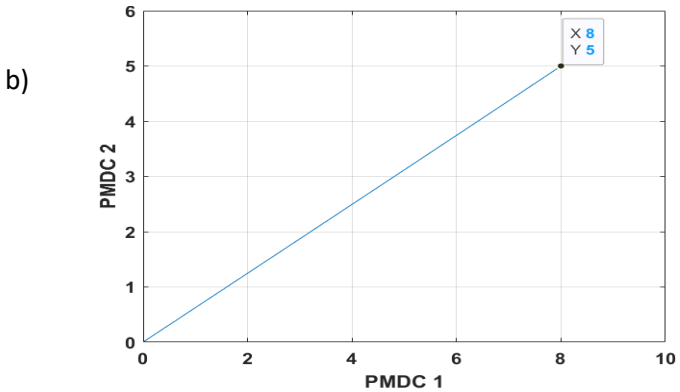

Fig. 10 (a) Actual position for two PMDC motors at no–load, (b) Final position in the X – Y graph, (c) Actual velocity at no –load

2- Single input position reference at load case.

As shown in Fig. 11 (a) the load is applied in the twentieth second and noticed a very small deviation from the reference position about 0.021 rad, after that, the system returned to steady-state. While Figure 11 (b) shows a very small deviation from the reference velocity, and after two seconds, the system returned to steady-state. The system does not affect after applying the full load and both PMDC motors reached the required position (8,5) rad at the same time, as shown in Figure 11 (c).

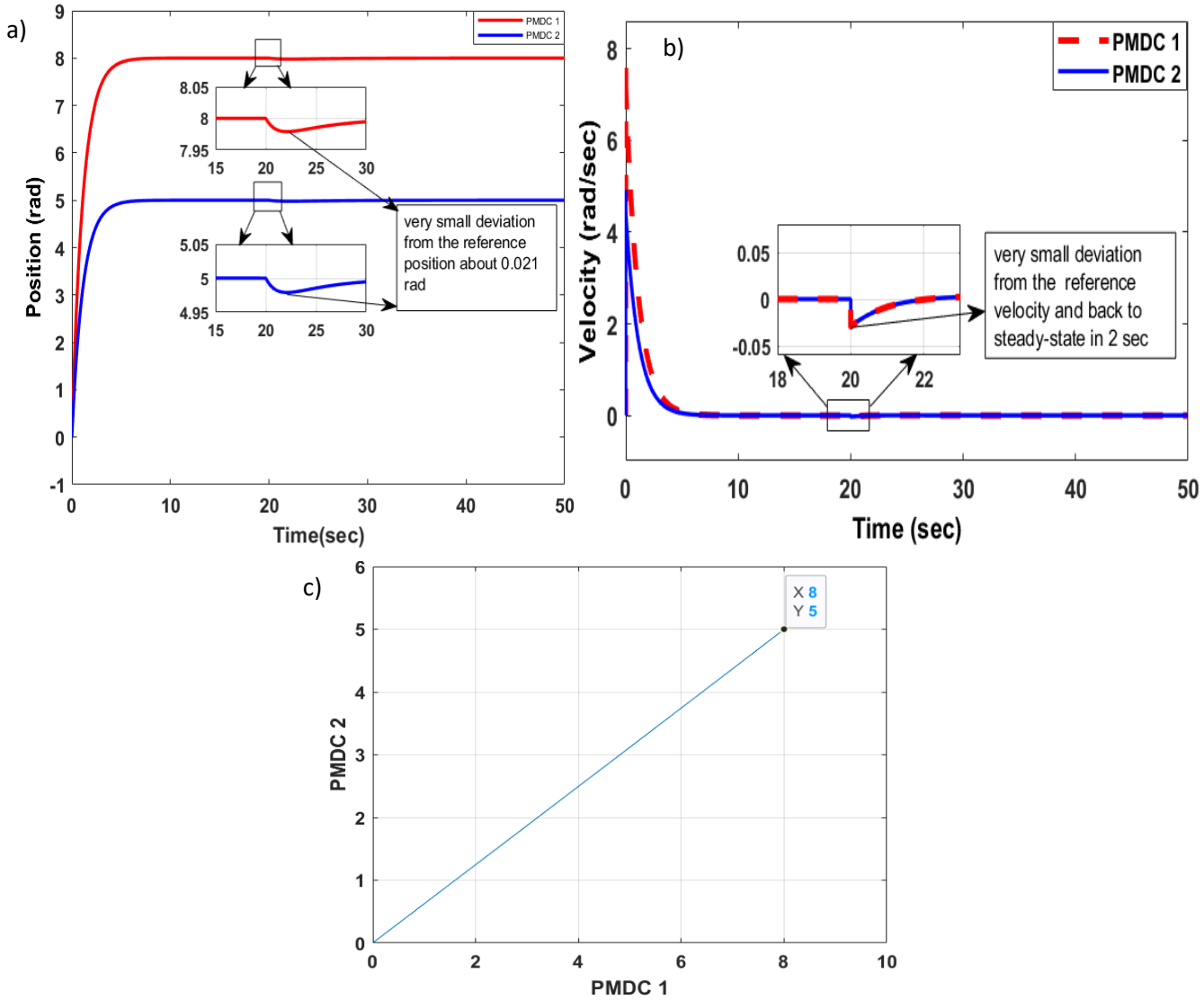

Fig. 11 (a) Actual position after a full load is applied, (b) Actual velocity after a full load is applied, (c) Final position in the X – Y graph at load case

3- Multi-input position reference at no-load case.

In this case, multiple high-value reference positions were entered for both PMDC motors. The reason for entering these high values is to ensure that the motors rotate more than once to reach the specified position.

Figure 12(a) shows the movement of the PMDC 1 motor on the x-axis to reach the specified positions (30, 50, 90) rad, respectively. While the PMDC 2 motor moves on the Y-axis to reach the specified position (70, 40, 80) rad, respectively. As a result, both PMDC motors will reach the specified positions on the X-Y graph at the same time, and this is an indication of the accuracy of the position and velocity controllers and the precise synchronization controller as shown in Figure12(b) and Table 5.

In addition, a very small deviation from the reference position about 0.0002 rad is observed when Both motors reach the first position.

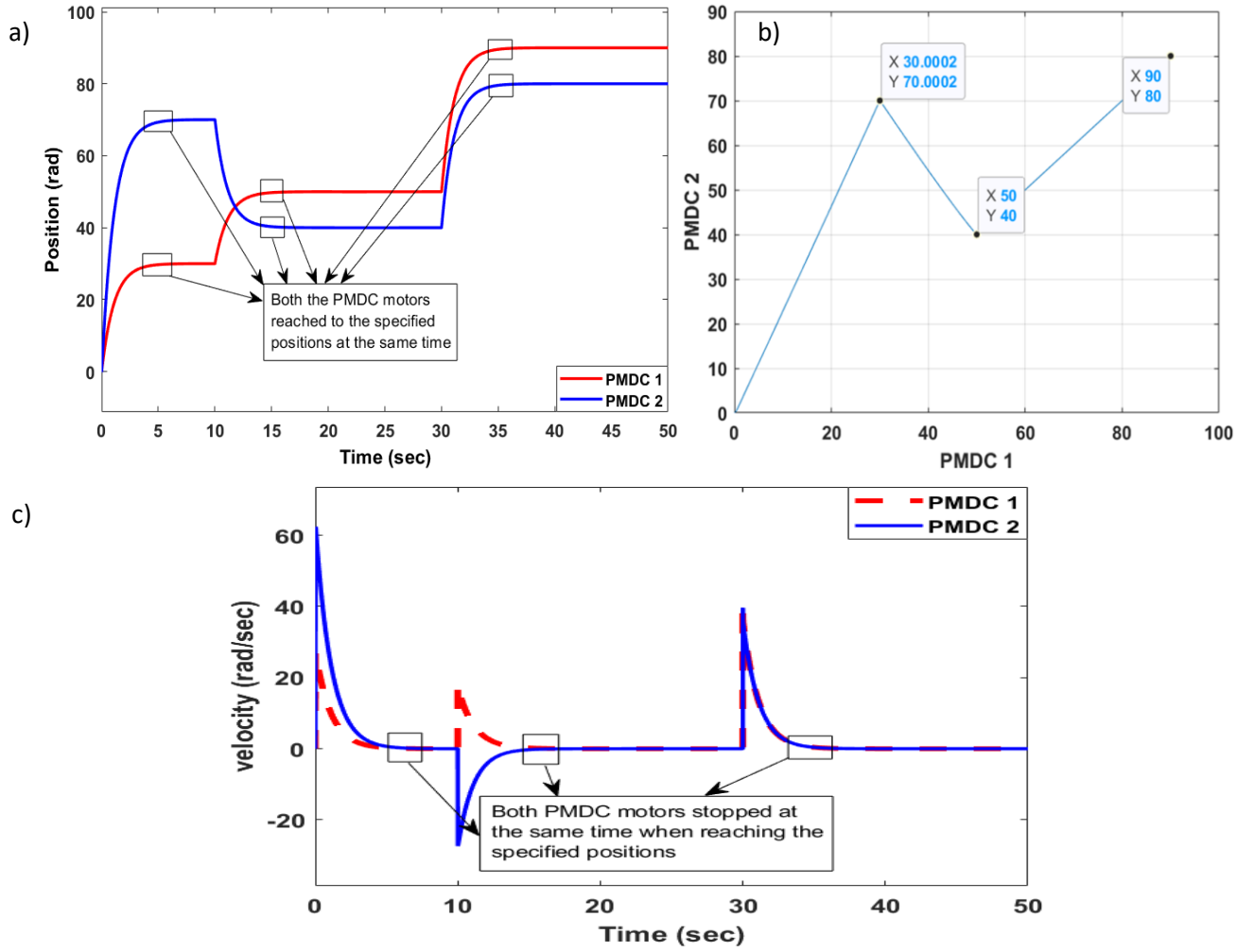

Fig. 12 (a) Multi-input Actual positions at no-load case, (b) Final positions in the X – Y graph, (c) Actual velocities for two PMDC motors at no –load

Table 5 P Actual, Final, and deviation positions on the axes

Actual positions for PMDC 1 on X-axis (rad)	Actual positions for PMDC 1 on Y-axis (rad)	Final positions on X-Y graph (rad)	Deviation value from the required position (rad)
30	70	30,70	0.0002
50	40	50,40	0
90	80	90,80	0

Figure 12(c) represents the rotation velocity of both motors, as these motors stop at the same time when they reach to the first required position, and then they move to the other position, and so on.

The negative velocity means that the motor has moved from a higher position to a lower position, and thus the motor's rotation will be reversed in the opposite direction.

4- Multi-input position reference at load case.

As in the case of single input, the full load is applied to the system at the twentieth second, where a small deviation from the reference position of both PMDC motors was observed during the applied load by 0.021 rad. Then the system returned to a steady-state as shown in Figure 13(a). While Figure 13(b) shows the actual velocity of the motors with a very small overshoot, and after two seconds the system returns to steady-

state. In the end, both PMDC motors reach the required positions without being affected by applied load, as shown in Table 4 and also in Figure 13(c).

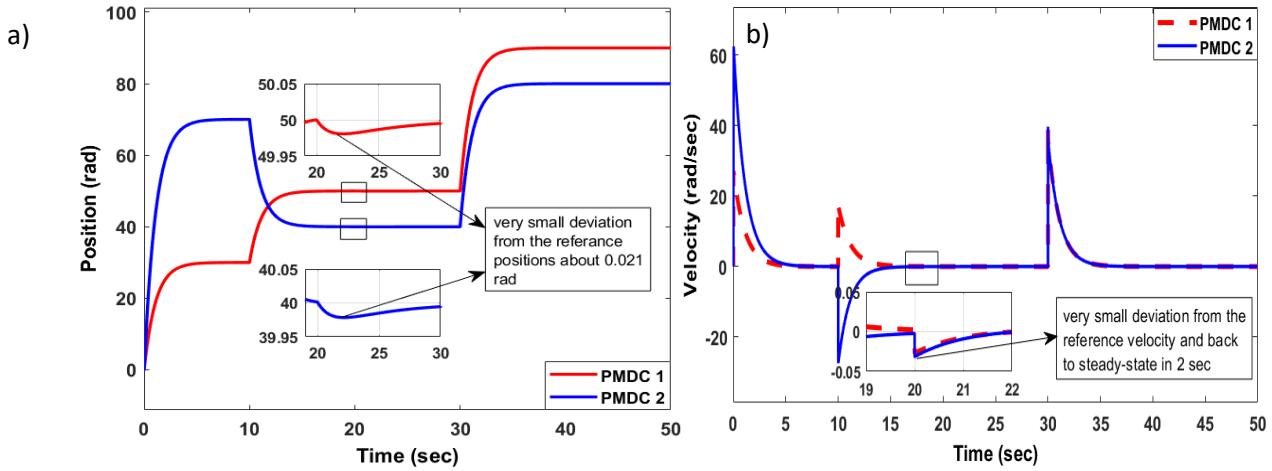

Fig 13(a) Multi-input Actual positions at load case Fig 13(b) Actual velocities at load case

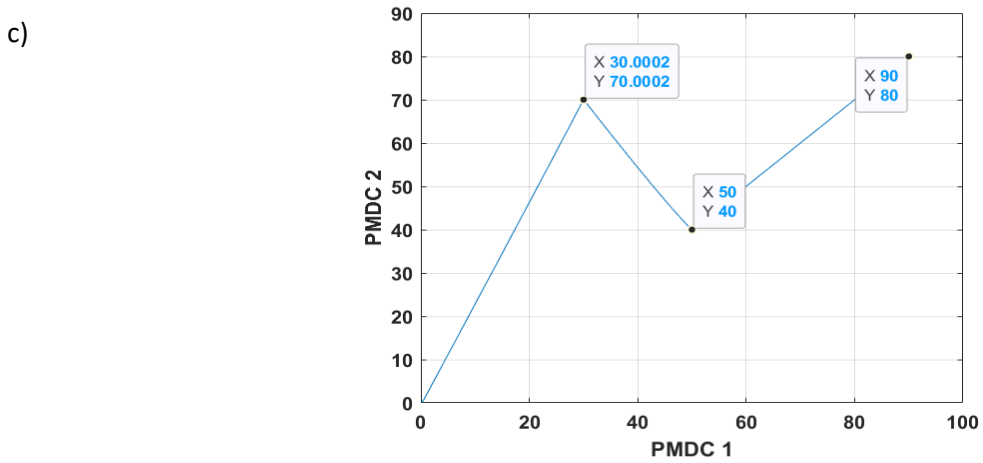

Fig. 13 (a) Multi-input Actual positions at load case, (b) Actual velocities at load case, (c) Final positions in the X – Y graph

Figures 14(a) and 14(b) represent the Actual position of each PMDC motor with its reference, where an accurate tracking trajectory is observed, which is an indication of the durability of the cascade controller.

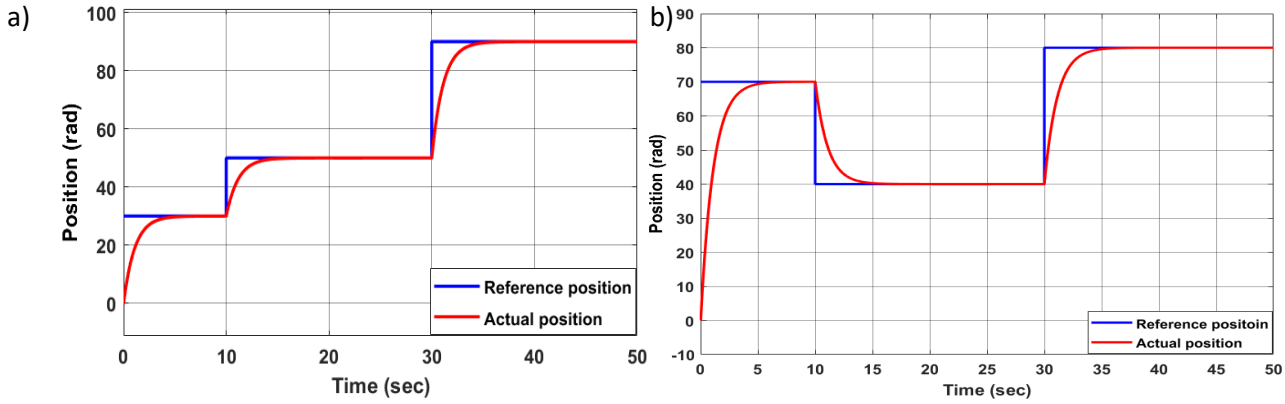

Fig. 14 (a) Reference and Actual position for PMDC 1, (b) Reference and Actual position for PMDC 2

Finally, the goal of synchronization is achieved, which is $\varepsilon p = 0$, as seen in figure 15 the value of the synchronization error in the case of one input for both PMDC motors.

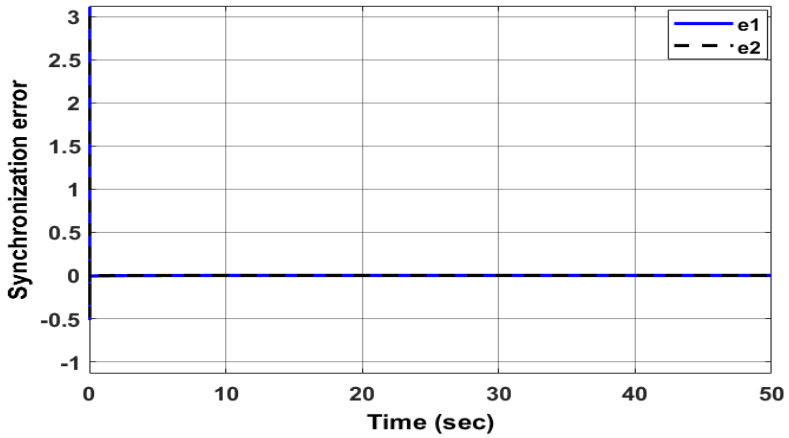

Fig. 15 Synchronization error between PMDC1 and PMDC 2

6. Conclusion

In this paper, a cascade controller is designed to control the velocity and position of two PMDC motors, in addition to using the cross-coupling technique to connect the two motors with each other and control the precise synchronization of its movement. The simulation results showed high accuracy to reach the required positions at a regular velocity with accurate synchronization of the movement on the axes. The system was tested in multiple cases such as loading and non-loading, in addition to applying one reference position or multiple reference positions to ensure that the motors rotated more than once, as the results also proved that the system did not affect applying the full load and reaching the desired final positions on the X-Y graph. This work can be implemented in real-time, taking into account the dynamic equations of the used system.

Reference

[1] K. Wu, C. Krewet, and B. Kuhlenkötter, “Dynamic performance of industrial robot in corner path with CNC controller,” Robot. Comput. Integr. Manuf., vol. 54, pp. 156–161, 2018.

[2] T. A. Bigelow, Electric Circuits, Systems, and Motors. Springer, ch 5 .p 148, 2020.

[3] P. C. Krause, O. Wasynczuk, S. D. Sudhoff, and S. Pekarek, Analysis of electric machinery and drive systems, vol. 2. Wiley Online Library, 3ed ,ch 10 pp. 396-397, 2002.

[4] B. L. Theraja, A textbook of electrical technology. S. Chand Publishing, ch 39 p 1549, 2008.

[5] W. H. Ali, M. N. O. Sadiku, and S. Abood, Fundamentals of Electric Machines: A Primer with MATLAB: A Primer with MATLAB. CRC Press, ch 11 p 335,2019.

[6] J. Bae, K. Cho, and D.-H. Lee, “Parallel Position Control Scheme of Permanent Magnet DC Motors with a Low-Resolution Sensor,” in 2020 IEEE International Conference on Industrial Technology (ICIT), 2020, pp. 199–204.

[7] Z. Adel, A. A. Hamou, and S. Abdellatif, “Design of Real-time PID tracking controller using Arduino Mega 2560for a permanent magnet DC motor under real disturbances.,” in 2018 International Conference on Electrical Sciences and Technologies in Maghreb (CISTEM), 2018, pp. 1–5.

[8] M. F. Cankurtaran and A. E. Kocamis, “Sensorless Speed Control of PMDC Motor with Cascade PI Controller,” in 2019 International Symposium ELMAR, 2019, pp. 203–206.

[9] T. N. Gücin, M. Biberoğlu, B. Fincan, and M. O. Gülbahçe, “Tuning cascade PI (D) controllers in PMDC motor drives: A performance comparison for different types of tuning methods,” in 2015 9th International Conference on Electrical and Electronics Engineering (ELECO), 2015, pp. 1061–1066.

[10] L. Wang, PID Control System Design and Automatic Tuning Using MATLAB/Simulink. John Wiley & Sons, chp 7 p 209, 2020.

[11] G. L. Raja and A. Ali, “Series cascade control: An outline survey,” in 2017 Indian Control Conference (ICC), 2017, pp. 409–414.

[12] Y. Xie, J. Jin, X. Tang, B. Ye, and J. Tao, “Robust cascade path-tracking control of networked industrial robot using constrained iterative feedback tuning,” IEEE Access, vol. 7, pp. 8470–8482, 2018.

[13] C. Zhang, J. He, L. Jia, C. Xu, and Y. Xiao, “Virtual line-shafting control for permanent magnet synchronous motor systems using sliding-mode observer,” IET Control Theory Appl., vol. 9, no. 3, pp. 456–464, 2015.

[14] H. M. Guzey, A. Dumlu, N. Guzey, and A. Alpay, “Optimal synchronizing speed control of multiple DC motors,” in 2018 4th International Conference on Optimization and Applications (ICOA), 2018, pp. 1–5.

[15] P. Zhang and Z. Wang, “Improvements of direct current motor control and motion trajectory algorithm development for automated guided vehicle,” Adv. Mech. Eng., vol. 11, no. 2, p. 1687814018824937, 2019.

[16] Y. Xiao, Y. Pang, X. Ge, and J. Sun, “Synchronous control for high-accuracy biaxial motion systems,” J. Control Theory Appl., vol. 11, no. 2, pp. 294–298, 2013.

[17] K. Ishizaki, B. Sencer, and E. Shamoto, “Cross Coupling Controller for Accurate Motion Synchronization of Dual Servo Systems.,” IJAT, vol. 7, no. 5, pp. 514–522, 2013.

[18] V. Mhase, R. Sudarshan, O. Pardeshi, and P. V Suryawanshi, “Integrated speed–position tracking with trajectory generation and synchronization for 2–axis DC motion control,” Int. J. Eng. Res. Dev., vol. 1, no. 6, pp. 61–66, 2012.

[19] S.-M. Wang, R.-J. Wang, and S. Tsooj, “A new synchronous error control method for CNC machine tools with dual-driving systems,” Int. J. Precis. Eng. Manuf., vol. 14, no. 8, pp. 1415–1419, 2013.

[20] N. K. Sinha and P. M. Tiwari, “Multiple motor synchronization using nonlinear PID control,” in 2017 3rd International Conference on Advances in Computing, Communication & Automation (ICACCA)(Fall), 2017, pp. 1–6.

[21] M. Namazov and O. Basturk, “DC motor position control using fuzzy proportional-derivative controllers with different defuzzification methods,” 2010.

[22] R. C. Dorf and R. H. Bishop, Modern control systems. Pearson,12ed , ch 2 pp 71-72, 2011.

[23] K. T. Chau and Z. Wang, Chaos in electric drive systems: analysis, control and application. John Wiley & Sons, ch 2 p 52, 2011.

[24] N. Mohan, Electric drives, chp4 p5 & ch8 pp7-8 & ch8 p19. 2003.

[25] H. Huang, Q. Tu, C. Jiang, L. Ma, P. Li, and H. Zhang, “Dual motor drive vehicle speed synchronization and coordination control strategy,” in AIP Conference Proceedings, 2018, vol. 1955, no. 1, p. 40005.

[26] D. Sun, Synchronization and control of multiagent systems. CRC Press, ch2& ch3 pp 27-34, 2018.

[27] S. Arora and S. Singh, “Butterfly optimization algorithm: a novel approach for global optimization,” Soft Comput., vol. 23, no. 3, pp. 715–734, 2019.

[28] A. Latif, S. M. Hussain, D. C. Das, and T. S. Ustun, “Optimum Synthesis of a BOA optimized novel dual-stage PI-(1+ ID) controller for frequency response of a microgrid,” Energies, vol. 13, no. 13, p. 3446, 2020.